



Atmospheric Boundary Layer in the Atlantic: the desert dust impact

Ioanna Tsikoudi^{1,2}, Eleni Marinou¹, Maria Tombrou², Eleni Giannakaki², Emmanouil Proestakis¹, Konstantinos Rizos¹, Ville Vakkari^{3,4}, and Vassilis Amiridis¹

¹National Observatory of Athens, IAASARS, Greece

²Department of Physics, National and Kapodistrian University of Athens, Greece

³Finnish Meteorological Institute, Finland

⁴Atmospheric Chemistry Research Group, Chemical Resource Beneficiation, North-West University, Potchefstroom, South Africa

Correspondence: Ioanna Tsikoudi (jtsik@noa.gr)

Abstract. We investigate the dynamics of the atmospheric Boundary Layer (BL) over the Atlantic Ocean, with a focus on the region surrounding Cabo Verde during the Joint Aeolus Tropical Atlantic Campaign (JATAC) and the ASKOS experiment, using a combination of ground-based PollyXT and Doppler lidars, satellite lidar data from Cloud-Aerosol Lidar and Infrared Pathfinder Satellite Observations (CALIPSO), radiosondes, and the model outputs of the Integrated Forecasting System (IFS) of the European Centre for Medium-Range Weather Forecasts (ECMWF). The comparison of CALIPSO lidar results with ECMWF/IFS reanalysis for 2012-2022, revealed strong correlations for BL top over open ocean regions but weaker relation over dust-affected areas closer to the African continent. In these regions, space lidar indicated lower BL tops during daytime than those estimated by ECMWF/IFS. Observations in Cabo Verde highlight distinctive Marine Atmospheric Boundary Layer (MABL) characteristics, such as limited diurnal evolution, but also show the potential for BL heights to reach up to 1 km, driven by factors like strong winds that increase mechanical turbulence. Additionally, the challenges in estimating the BL height using lidar-derived aerosol mixing height versus profiling of meteorological parameters acquired from radiosondes are illustrated, examining cases with strong and weaker inversions that affect the vertical mixing and the penetration of dust particles within the BL. The findings underline the need for further improvements in the ECMWF/IFS reanalysis model towards capturing the complex interactions between marine and dust-laden air masses over the Atlantic, which are essential for constraining the dynamic processes in BL and aerosol-cloud interactions.

1 Introduction

The atmospheric Boundary Layer (BL) is characterized by complex interactions between surface-driven forces and meteorological conditions, which determine its height, structure, and the degree of turbulent mixing within (Stull, 1988). BL dynamics vary considerably across different environments, presenting challenges for weather modeling and prediction, especially in transitional zones like those between deserts and oceans (Seibert et al., 2000; Li et al., 2017).

Monitoring the BL top reliably is a challenge, particularly in heterogeneous environments where traditional observation methods may fall short. Lidar systems have proven valuable for continuous profiling of aerosol and atmospheric structures, as their high vertical resolution enables detailed monitoring of BL height (Wiegner et al., 2006; Baars et al., 2008). Yet, automatic



identification of the BL top from lidar data is challenging in complex areas, because BL structures can be influenced by surface type, time of day, and atmospheric stability (Tsikoudi et al., 2022). Up to now, lidar-based BL retrievals showed very good performance on relatively predictable areas with known BL patterns, such as open land surfaces or stable atmospheric conditions (Tsaknakis et al., 2011; Seidel et al., 2012). Expanding lidar BL retrievals to more complex environments, is an ongoing challenge especially when it comes to oceanic and coastal BLs where ground-based observation sites are limited.

Over the open Atlantic, the Marine Atmospheric Boundary Layer (MABL) is typically shallow and influenced by the relatively constant sea surface temperature, while boundary layers in coastal and island regions experience terrestrial-marine interactions that increase their variability (Garratt, 1994; Wood, 2012). Few studies over years have addressed the detection and analysis of MABL using lidar data, largely due to practical and observational challenges over the ocean (e.g. Atlas et al. 1986; Flamant et al. 1997; Pena et al. 2015). Given these constraints, satellite observations, such as those provided by the Cloud-Aerosol Lidar and Infrared Pathfinder Satellite Observations (CALIPSO) mission, have become essential for studying lower troposphere characteristics over remote regions, offering a means to improve understanding of these complex systems.

The general circulation over the tropical Atlantic is dominated by the Inter-Tropical Convergence Zone (ITCZ) and affected by the presence of the Saharan Air Layer (SAL). The SAL is a typically warm and dry air layer that frequently occurs at large scales in the tropical North Atlantic Ocean and can reside up to 5 km in altitude, often accompanied by dust aerosols (Carlson and Prospero, 1972; Dunion and Velden, 2004; Wu, 2007). The ITCZ, migrates seasonally between the northern and southern tropics, influencing rainfall and convective activity, creating conditions conducive to both the formation of clouds and the aerosol convection over the Atlantic (Zhou et al., 2020). In tandem, the SAL, comprising of hot, dry air laden with desert dust from the Sahara, moves westward across the Atlantic Ocean, especially in summer, driven by the prevailing trade winds (Prospero and Mayol-Bracero, 2013) and has consequences on the surface radiation budget (Evan et al., 2009; Yu et al., 2006). These circulation patterns are key in transporting dust from Africa to the Atlantic, affecting the radiative balance and potentially impacting cloud formation, atmospheric stability, and therefore BL behavior in the region (Sun and Zhao, 2020).

A typical characteristic of the eastern sides of the Atlantic, is that the air subsiding into the subtropical north-east Atlantic is warmer and drier than the air that has been in contact with the relatively cold ocean surface influenced by upwelling, and a strong inversion forms at the interface of the two air masses (Hanson, 1991). As such, transported desert dust from Africa introduce another layer of complexity in tropospheric dynamics and clouds activity by altering radiation budget, atmospheric stability, and moisture distribution (e.g. Marinou et al. 2021; Ansmann et al. 2017; Marsham et al. 2008). This dual effect of dust—scattering and absorbing solar radiation while in the same time serving as cloud condensation and ice nucleation nuclei (CCN/IN)—leads to competing influences on the BL (e.g radiative cooling can suppress turbulent mixing, yet CCN activation can lead to increased cloud cover and associated feedback on surface radiation). These processes have been observed to influence the vertical structure and stability of the BL, but their overall impact on BL dynamics is still not fully understood.

Accurately representing BL-aerosol interactions in climate and chemical transport models is crucial because these processes affect surface conditions and large-scale atmospheric circulation (Menut et al., 2009; Pérez et al., 2006; Tombrou et al., 2015, 2007). Gaps in observational data over complex environments, such as the dust-laden, desert-ocean transition zone in the Atlantic, limit the model's ability to accurately capture BL evolution and aerosol influences (Rémy et al., 2019, 2021;



Kallos et al., 2007). The need for observational data to validate and refine these models is high, especially given the impacts on cloud formation, energy distribution, and surface-air interactions. Addressing these gaps through both ground-based experimental campaigns such as Joint Aeolus Tropical Atlantic Campaign (JATAC) and satellite sensors such as space Lidars can significantly enhance understanding and modeling of BL processes in regions of critical climatic importance. In addition to investigating BL-aerosol interactions, this study aims to improve BL top detection methods in diverse and complex environments. By addressing challenges inherent to automated BL detection, particularly in areas affected by aerosols and variable atmospheric conditions, this work contributes to the development of more robust methods for BL identification.

The structure of this paper is as follows: Section 2 provides an overview of the datasets and methods used, including ground-based lidar, space lidar, radiosonde data, and model outputs. Section 3 examines the BL characteristics across different environments, beginning with the Atlantic Ocean (Area 1) and the ocean-desert transition zone (Area 2), before focusing on Cabo Verde, where dust interactions with the BL are investigated. Finally, Section 4 presents the main conclusions of this study.

2 Framework for Data Sources and Analysis

This study utilizes data from the ASKOS Campaign (Marinou et al., 2023), which is the ground-based component of the JATAC organised by the European Space Agency (ESA). ASKOS took place at the Ocean Science Centre Mindelo (OSCM), at the island of São Vicente, Cabo Verde, during 2021-2022.

2.1 Datasets

For this analysis, we use the comprehensive ASKOS dataset that, among others, includes active remote sensing observations and radiosonde datasets that are crucial for understanding atmospheric dynamics in the region. More specifically, radiosonde profiles, ground-based PollyXT lidar and Wind Doppler lidar measurements as well the LIVAS (Lidar climatology of Vertical Aerosol Structure for space-based lidar simulation studies) Climate Data Record (CDR) (Amiridis et al., 2015) using CALIPSO are examined. Additionally, the measurements-derived BL is compared to the ERA5 Re-Analysis dataset from Integrated Forecasting System (IFS) of the European Centre for Medium-Range Weather Forecasts (ECMWF), at $0.25^\circ \times 0.25^\circ$ resolution.

2.1.1 Groundbased Lidar

The ground-based PollyXT Raman Lidar (Engelmann et al., 2016), consists of a compact, pulsed Nd:YAG laser, emitting at 355, 532, and 1064 nm at a 20 Hz repetition rate, with the laser beam pointed into the atmosphere at an off-zenith angle of 5° . The backscattered signal is collected by a Newtonian telescope with a 0.9m focal length, acquiring profiles with a vertical resolution of 7.5 m, and a temporal resolution of 30 s. The system was operated by TROPOS during the ASKOS Campaign, providing data coverage for the entire campaign. Figure 1 presents PollyXT measurements, conducted during the ASKOS Campaign. Specifically, the attenuated backscatter coefficient of the 1064 nm channel (Att BSC, Fig. 1-left) is examined to derive the BL top, and the volume linear depolarization ratio (VLDR, Fig. 1-right) is investigated to infer the aerosol shape.



On that day, the closest CALIPSO trajectory point was at 4:07 UTC, located approximately 240 km east of the Mindelo site.

90 The white points in the attenuated backscatter indicate the presence of clouds and were not included in the BL analysis.

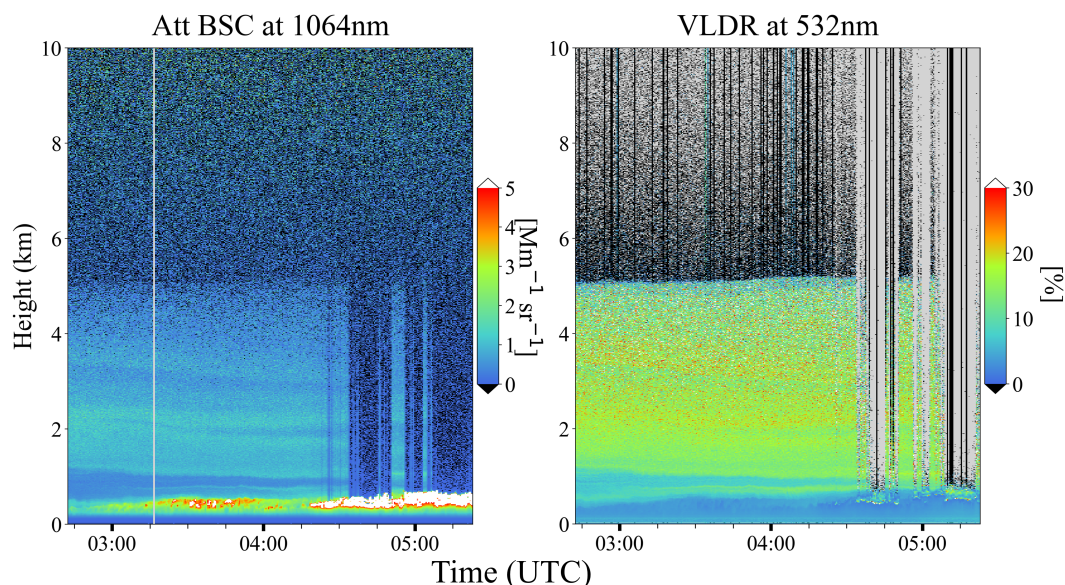


Figure 1. Ground-based PollyXT Lidar at Mindelo (16.87°N, 24.99°W), Cabo Verde, on the 10th of September, 2021, depicting the attenuated backscatter coefficient (Att Bsc) at 1064 nm (left), and volume linear depolarization ratio (VLDR) at 532 nm (right).

Additionally, complementary data from a Halo Photonics Stream Line scanning Doppler lidar were used to examine the horizontal wind speed and direction, as well as the vertical wind component. This lidar is a 1.5 μm pulsed Doppler lidar with a heterodyne detector (Pearson et al., 2009). The Doppler lidar has a range resolution of 48 m and measures the attenuated aerosol backscatter and Doppler velocity along the beam direction. Horizontal wind profiles were retrieved from a velocity azimuth display (VAD) scan with 12 azimuthal angles at 60° elevation angle every 15 minutes. Otherwise, the Doppler lidar operated in vertical stare mode, retrieving vertical wind profile time series.

The Doppler lidar data was post-processed according to Vakkari et al. (2019) and a signal-to-noise ratio (SNR) threshold of 0.005 was applied to the vertically-pointing measurements. Turbulent kinetic energy (TKE) dissipation rate profiles were calculated from the vertically-pointing data using the method by O'Connor et al. (2010). Instrumental noise was calculated from signal-to-noise ratio according to Pearson et al. (2009) and subtracted from the vertical wind variance time series before the TKE dissipation rate calculation. To estimate mixed layer height (MLH) from the TKE dissipation rate profiles a threshold of $10^{-4} \text{m}^2 \text{s}^{-3}$ was applied, similar to previous studies (e.g. Vakkari et al., 2015).

2.1.2 Space lidar: CALIPSO–CALIOP

Towards investigating the dynamics of the BL over the Atlantic Ocean, observations of the Cloud–Aerosol Lidar with Orthogonal Polarization (CALIOP; Hunt et al. 2009), the primary instrument on board the joint National Aeronautics and Space



Administration (NASA) and Centre National D'Études Spatiales (CNES) Cloud–Aerosol Lidar and Infrared Pathfinder Satellite Observation (CALIPSO) mission (Winker et al., 2010), are extensively used. More specifically, CALIOP provided as integrated component of the Afternoon-Train constellation of polar-orbit sun-synchronous satellites (Stephens et al., 2018), profiles of aerosols and clouds along the CALIPSO orbit-path between June 2006 and August 2023. In the framework of the study, CALIOP Level 2 (L2) Version 4 (V4) aerosol profiles (APro) of backscatter coefficient at 532 nm and particulate depolarization ratio at 532 nm are used, provided at uniform 5 km horizontal resolution and 60 m vertical resolution for the altitudinal range between -0.5 and 20.2 km above mean sea level (a.m.s.l.) are used, for the domain encompassing the broader North Atlantic Ocean - Western Saharan Desert and for September 2021. Prior implementation of CALIOP optical products, rigorous quality assurance procedures are applied (Marinou et al., 2017; Proestakis et al., 2024), following also the quality controls adopted towards the generalization of the official CALIPSO Level 3 (L3) products (Winker et al., 2013; Tackett et al., 2018). Towards this objective, the most aggressive quality control procedure applied in the framework of the study is the cloud-free condition, removing the entire L2 profiles when detected atmospheric layers (Vaughan et al., 2009) along the CALIPSO orbit-path are classified as clouds in the feature-type classification algorithm (Liu et al., 2009; Zeng et al., 2019). Figure 2 provides an indicative example of the considered CALIOP observations and products, and more specifically the Feature Type (Fig.2 top left) product and the profiles of particulate depolarization ratio at 532 nm (Fig.2 top right), total backscatter coefficient at 532 nm (Fig.2 bottom left), and quality-assured total backscatter coefficient at 532 nm (Fig.2 bottom right), along the CALIPSO overpass on the 10th of September 2021.

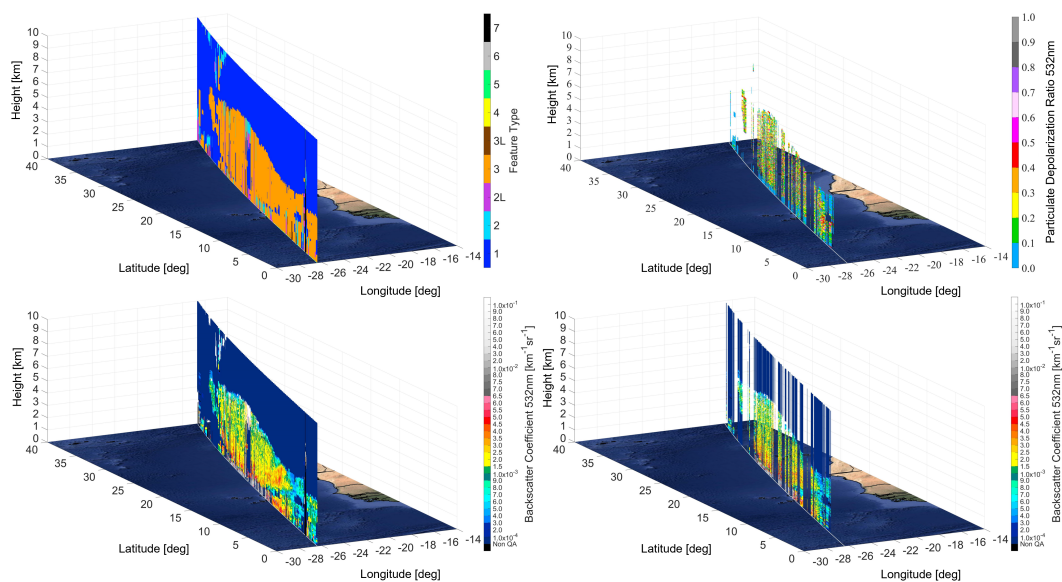


Figure 2. CALIPSO nighttime overpass in the ESA-ASKOS campaign region of interest in the proximity of Cabo Verde on the 10th of September, 2021, depicting the Feature Type (top left), particulate depolarization ratio at 532 nm (top right), total backscatter coefficient at 532 nm (bottom left), and the quality-assured total backscatter coefficient at 532 nm (bottom right).



2.1.3 Radiosondes and models

Radiosonde profiles were analyzed to examine the dynamic structure of the lower troposphere and to evaluate the remote sensing measurements conducted during the ASKOS Campaign. The GRAW DFM-09 radiosondes were launched to provide real-time, high-resolution measurements of temperature, humidity, and wind, which are essential for identifying the BL key characteristics, such as height, stability, and thermodynamic properties. The sensors were equipped with a GPS receiver and transmit data via a radiofrequency link to the ground station.

The measurements-derived BL height was compared to values obtained from the ERA5 Reanalysis dataset, produced by the ECMWF/IFS. The ERA5 data, available at a horizontal resolution of $0.25^\circ \times 0.25^\circ$ with 137 vertical levels (Vogelezang and Holtslag, 1996), offers a consistent representation of atmospheric conditions. The BL height in ERA5 is determined according to ECMWF (2017), Chapter 3, incorporating thermodynamic criteria.

Additionally, Hybrid Single-Particle Lagrangian Integrated Trajectory (HYSPLIT) is employed to analyse the backward trajectories of air masses arriving at the site of the ASKOS Campaign, Mindelo, Cabo Verde. This model estimates the tracking of air parcels over time, providing valuable information about the origins of the air parcels and their potential interactions with dust and other atmospheric constituents (Rolph et al., 2017). By identifying these pathways, a clearer understanding of the sources and transport mechanisms of the the atmospheric conditions at Cabo Verde can be established.

2.2 Boundary Layer top retrieval Methods

To retrieve the BL heights from the lidar measurements, the Wavelet Covariance Transform (WCT) and the Gradient Method are applied (Brooks, 2003; Li et al., 2021) on the cloud-free backscatter coefficient profiles of the CALIOP (Fig. 2-bottom right) and ground-based PollyXT lidar (Fig. 1, left) for the channels of 532 and 1064 nm respectively. For the radiosonde data, layer detection is achieved with the gradient method. In some cases, detecting the BL top relies on visual inspection to accurately locate the inversion cap, especially in cases where automated methods might miss subtle features. Figure 3 shows profiles of the backscatter coefficient at 1064 nm from ground-based PollyXT (left), of the Relative Humidity (RH) from radiosonde (middle) and backscatter coefficient at 532 nm from CALIPSO satellite lidar (right) from the 23rd of September 2022, around 19:30 UTC. The grey lines represent the result of the method applied for detecting BL top, namely WCT method for PollyXT Lidar and Gradient method for the rest two. A local maximum of the wavelet profile for WCT method, and a local minimum of the gradient for the gradient method, represent steep reduction in the investigated signal (red dashed lines).

Several significant challenges arise when studying the BL with lidars (both ground-based and satellite), particularly in complex environments. For a satellite-based lidar like CALIOP, the signal can become highly attenuated as it approaches the Earth's surface, due to the existence of clouds above the BL. This can compromise the reliability of detecting lower tropospheric features and lead to inaccurate identification of the BL top. To mitigate this, only cloud-free profiles were selected to ensure data quality, though this restriction reduces the dataset and introduces observational limitations. Additionally, in marine environments, cumulus clouds frequently form at the BL top, which can serve as a useful, albeit indirect, marker for BL height for ground-based lidars that can detect the cloud base. Moreover, if a thin cumulus cloud is present above the BL

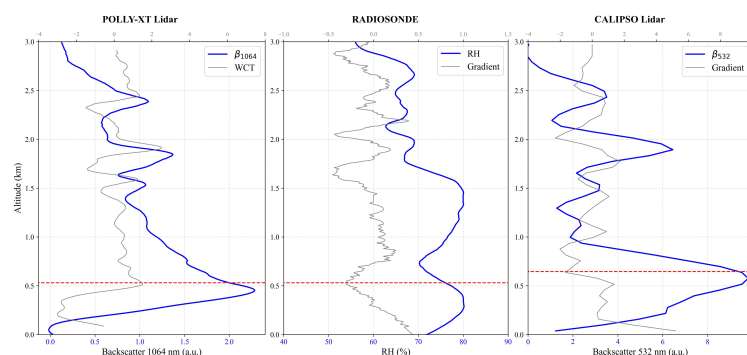


Figure 3. 23rd September 2022, around 19:30 UTC: Profiles of atmospheric variables and their corresponding detection methods for determining the boundary layer (BL) top. The blue lines represent the observed signals, while the grey lines correspond to the applied methods for BL top detection. Left: Backscatter coefficient at 1064 nm from the ground-based PollyXT lidar, Middle: Relative Humidity (RH) from radiosonde, and Right: backscatter coefficient at 532 nm from the CALIPSO satellite lidar. The selected BL top is highlighted by the red dashed lines.

top and allows partial laser penetration, the WCT may incorrectly identify the cloud's upper boundary as the BL top instead of the actual BL height. A similar issue occurs in the presence of dust layers, as the WCT detects reductions in the lidar signal caused by these layers. This can lead to misclassification of the dust layer boundaries as the BL top, complicating the accurate identification of the atmospheric structure. These limitations underscore the need for visual inspection to ensure accuracy in identifying the BL top in such settings, as automated methods may struggle to locate the correct layering.

3 Boundary Layer Characteristics in diverse environments

The characteristics of the BL during JATAC Campaign are examined across the contrasting environments depicted in Figure 4: over the Atlantic Ocean (blue rectangle - Area 1), within the ocean-desert transition zone (orange rectangle – Area 2), and at the area of São Vicente in Cabo Verde (red circle). The Sahara Desert and the Atlantic Ocean are characterized by distinct conditions in terms of weather, aerosol concentrations, and therefore atmospheric dynamics. These variations are anticipated to influence respectively the structure and evolution of BL in the Areas of Figure 4.

The lower troposphere above the Atlantic Ocean is rich in marine aerosols, and presents relatively stable meteorological conditions, typical for open-ocean broad-scale circulations (Croft et al., 2021). In contrast, the lower troposphere over the desert is characterized by high dust aerosol concentrations, intense solar heating, and variable atmospheric stability (Giménez et al., 2010). The border region between ocean and desert introduces an interaction zone where different aerosols co-exist in big concentrations, producing unique BL characteristics due to the convergence of these differing air masses. Moreover, the existence of SAL has an impact on the on the surface radiation budget (Evan et al., 2009) and hence on the sea surface temperature (SST). Foltz and McPhaden (2008) found that Saharan dust outflows at the Tropical North Atlantic, were consistently associated with a reduction in solar radiation, with approximately 35% of SST variability attributed to dust outbreaks, while



175 other SST cooling anomalies were linked to wind stress. The dust aerosol effect on SST depends on several factors, such as the temperature contrast between the dust layer and SST, the characteristics of the dust layer, concentration and altitude (Luo et al., 2021).

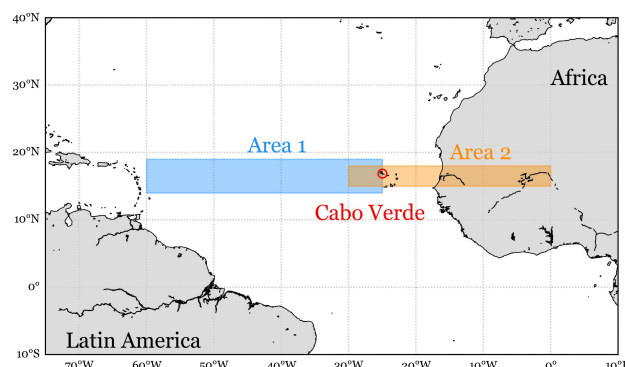


Figure 4. Map displaying the study areas for BL analysis: The blue rectangle (Area 1) represents the open-ocean Marine Atmospheric Boundary Layer (MABL) discussed in Section 3.1. The orange rectangle (Area 2) marks a transition zone at the ocean-desert interface, analysed in Section 3.2. The red circle is the ground-based measurements site at the Ocean Science Center Mindelo (OSCM) in Cabo Verde (3.3).

3.1 Analysis of Area 1: The BL in the Atlantic Ocean

The Atlantic Ocean is characterized by dynamic weather systems and cyclonic activity, incorporating continuous exchange of
180 heat and moisture between the sea surface and the adjacent air parcel (Schnitker, 1982). In open ocean areas such as Area 1, there is no direct interaction of the lower troposphere and the land, allowing for the development of a MABL. The MABL contains higher humidity levels and the airflow is smoother due to reduced friction from the water surface, comparing to land. Wind and temperature profiles in the MABL are mainly influenced by sea surface temperature, oceanic currents and large-scale atmospheric circulation.

185 In this section, we focus on the MABL characteristics within the blue rectangle of Area 1 (Figure 4). 10 years of CALIOP data (2012–2022) are examined, using only the profiles recorded in month September. By limiting the data to one month, we aim to achieve more homogeneous conditions to better capture the prevailing environmental characteristics (e.g. relatively consistent sea surface temperatures). Figure 5-left illustrates the conceptual trajectories of the CALIPSO satellite across the study area. The analysis targets cloud-free profiles measured within approximately 40 km around latitude 16.87° N, corresponding
190 to the latitude of ground-based measuring site in Cabo Verde, as represented by the red points in Figure 5-left. A total of 6392 nighttime and daytime profiles (conceptually indicated in green and purple, respectively) are analyzed across longitudes from 60° W to 25° W. The spatial range of 40 km is suitable for capturing representative MABL characteristics in the study area because the selected profiles are cloud-free and measured over the ocean surface, maintaining generally homogeneous conditions



of temperature, and humidity. For each profile, the derivative of the backscatter-coefficient profile at 532 nm is calculated (as
195 in Fig. 3-right) and the minima are constrained at the lower 3 km.

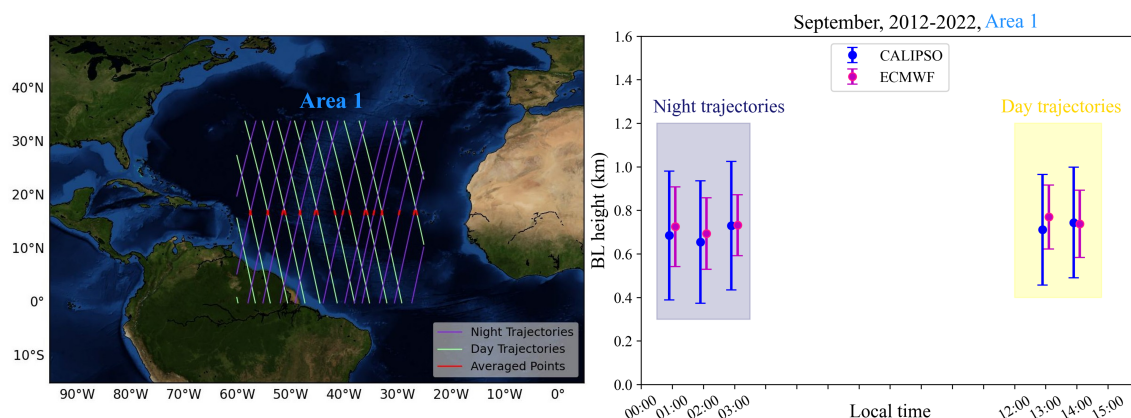


Figure 5. Left: Conceptual illustration of the trajectories of the CALIPSO satellite across the study area. Right: Comparison of BL top derived from CALIPSO (blue points) and ECMWF (magenta points) for 10 years (2012-2022) in Area 1.

The results of the MABL analysis from the space lidar data are compared with BL heights derived from the ECMWF/IFS dataset. To account for longitudinal time differences, each profile's measurement time is converted to local time based on its longitude. For each lidar profile, a temporally and spatially matched ECMWF point at the same local time is selected for direct comparison. The findings are presented in Figure 5-right.

200 The blue circles display the MABL top heights derived from CALIPSO profiles, averaged hourly in local time. The magenta points represent the corresponding hourly-averaged BL top heights from ECMWF. The data points are clustered within the 00:00–04:00 and 12:00–16:00 local time windows, because they correspond to CALIPSO's nighttime and daytime overpasses in the Atlantic region. The results show very good agreement overall, though lidar-derived BL heights carry greater uncertainty and sensitivity. This is expected, as uncertainties in the lidar profiles, occur not only from time averaging but also from the
205 gradient method used to derive heights from CALIOP profiles, which can be challenging to automate due to low signal to noise ratios especially during daytime. In contrast, the model is less sensitive to small-scale variations, as it provides an averaged representation over a relatively large grid (0.25° or 27.83 km around 16°N). The BL top in Area 1 under cloud-free conditions, is found to consistently range between 600 and 800 meters above sea level. Although uncertainties in deriving the BL and time averaging broaden this estimate, these findings align well with expected MABL behavior that typically do not show a
210 significant diurnal evolution.

3.2 Analysis of Area 2: The BL in the Ocean-Desert Transition Zone

Area 2, highlighted by the orange rectangle in Figure 4, spans within longitudes of 35°W-0°: from the eastern Atlantic Ocean to the Western Africa, including the region around Cabo Verde. This area lies at the interface of two significantly different



environments, as land and water interact differently with solar radiation due to their distinct heat capacities and reflective
 215 properties. On the West Africa land side, the lower troposphere directly interacts with the continental surface and the air is
 enriched with desert dust aerosols originating from the Sahara, where high temperatures, dry conditions, and strong winds
 are dominant. In contrast, the Eastern Atlantic Ocean side is predominantly influenced by marine aerosols within the lower
 troposphere, reflecting the ocean's stable, moisture-laden environment. In terms of heat capacity, land absorbs and releases heat
 quickly, leading to larger temperature fluctuations, while water absorbs energy more gradually, storing and slowly releasing it.
 220 These sharp contrasts in meteorological conditions and aerosol composition across the Area 2, are expected to have a notable
 impact on the BL structure.

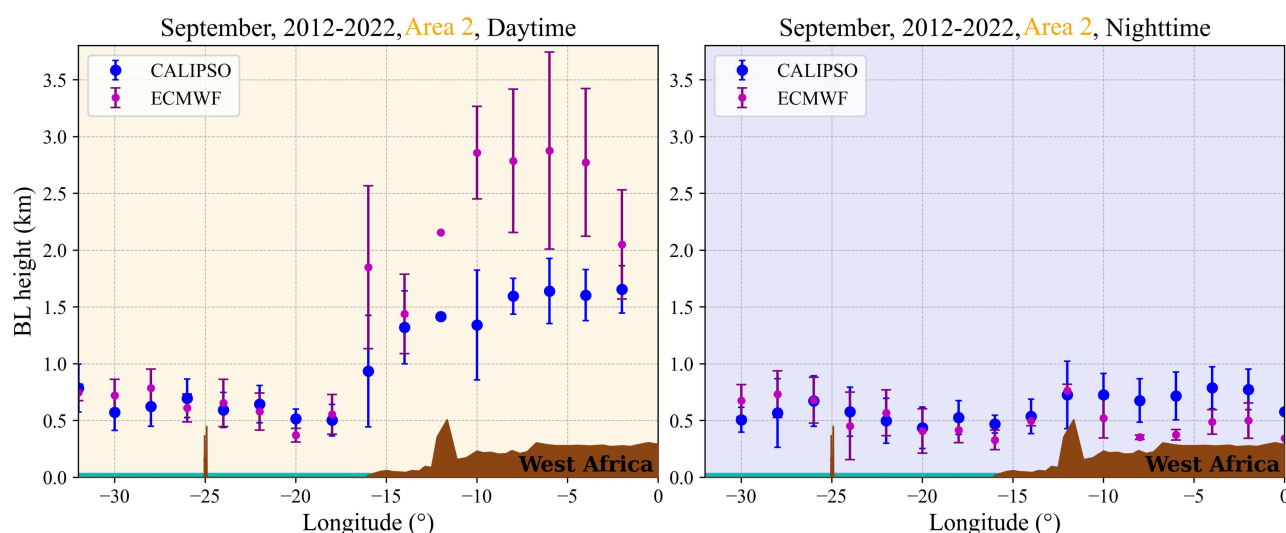


Figure 6. BL height along the latitude of 16.84°N for September 2012–2022 (Area 2), derived from CALIPSO lidar (blue points) and ECMWF model data (magenta points). CALIPSO trajectories were collocated with the nearest ECMWF model grid, and data were averaged over 2° longitudinal intervals. The error bars represent the variability in the BL height. The brown shaded region represents the topography of West Africa, indicating landmass and orographic features influence on the BL structure (sourced from Google Earth). The left figure illustrates daytime and the right illustrates nighttime trajectories.

For this analysis, similarly to section 3.1, cloud-free profiles were selected from the CALIPSO satellite lidar for September 2012–2022 to derive the BL top and are compared with the corresponding ECMWF data. Figure 6 presents the BL top results obtained from CALIPSO lidar measurements (blue points), and from the corresponding ECMWF points (magenta) along the
 225 cross-section at latitude 16.87° N (the latitude of the Mindelo observatory). The CALIPSO trajectories are divided into daytime (Fig. 6-left) and nighttime (Fig. 6-right) intervals after converting o local time, to highlight the distinct patterns of BL during different phases of the diurnal cycle.

Over the ocean surface, from 35° W to 17° W, the BL heights derived from CALIPSO and ECMWF data show good agreement for both daytime and nighttime trajectories, with values ranging from approximately 500 to 800 meters. This aligns



230 with the findings from section 3.1 (Area 1). However, discrepancies arise when examining the area above the African land, extending from 17° W to 0°. During the daytime, both the CALIPSO and ECMWF measurements show high BL heights, typical for continental and desert areas where the BL top is usually elevated (Garcia-Carreras et al., 2015). Notably, ECMWF reports significantly higher BL top than CALIPSO in this region. This could be attributed to the fact that CALIPSO in some cases detects the mixing layer height rather than the residual layer and the entrainment zone (Liu et al., 2018).

235 3.3 Focusing on Cabo Verde and JATAC/ASKOS

Cabo Verde is an archipelago in the eastern tropical Atlantic, with distinctive BL dynamics shaped by both the insular geography and the influence of surrounding mountains on airflow patterns. Specifically, the highest point is the Monte Verde (744m) on the eastern side, but there are also Caixa (535m) and Madeiral (680m) on the southern part, as well as Monte Cara (490 m) on the western part. Another geographical characteristic, is that Cabo Verde is situated directly in the path of frequent Saharan
240 dust transport, so the region is often impacted by large dust plumes originating from the African continent and crossing over the islands. These dust events vary significantly in intensity, sometimes accumulating right above the BL or penetrating into it, while at other times showing minimal impact due to lower dust loads.

The islands of Cabo Verde, are located nearly 1000 km from the West African coast. The region of São Vicente spans approximately 227 km², while the neighbouring (northern) island of Santo Antão covers around 785 km², creating an interface
245 where land and sea effects influence local atmospheric conditions. The origins of air drawn in to the trade winds arriving at Cape Verde are diverse depending on the season; from North America, the Atlantic, Arctic, European and African regions. During autumn, Cape Verde is situated in the direct transport pathway of easterly dust from Africa to the North Atlantic (Carpenter et al., 2010). These sea-air temperature contrasts, rough land surfaces, and fluctuating humidity contribute to a dynamic environment that reflects both marine and coastal BL characteristics.

250 To investigate the BL above Cabo Verde, we examine data from Radiosondes, ground-based PollyXT and Halo Lidar, CALIPSO and ECMWF/IFS model for September 2021 and 2022 (the intensive-measurements period of ASKOS). For this analysis, CALIPSO trajectories passing over the point of ground-based observations(16.87°N, 24.99°W) within a 300 km radius were carefully selected (Fig. 7, left). In Figure 7-right, the x-axis represents the BL top retrieved from CALIPSO ECMWF. The blue circles correspond to BL heights from ECMWF output, the red rectangles represent BL heights retrieved
255 from the PollyXT Lidar and the black hexagons represent MLH retrieved from the Halo Lidar. The PollyXT and Halo points are fewer because the instruments were not operational during several overpasses. Additionally, three collocated radiosonde measurements are depicted as green stars.

The black dashed line indicates the 1:1 line ($y=x$), representing perfect agreement between CALIPSO and the other datasets. The grey shaded area illustrates a $\pm 20\%$ error margin, while the cyan shaded region corresponds to a ± 100 m error margin,
260 providing a way to assess deviations from perfect correlation and evaluate whether the data points lie within an acceptable error range. From the analysis, 77% of the red points (PollyXT), 50% of the blue points (ECMWF) and 30% of the black points (Halo) fall within the grey shaded area, indicating agreement within 20% error when comparing with CALIPSO BL height.

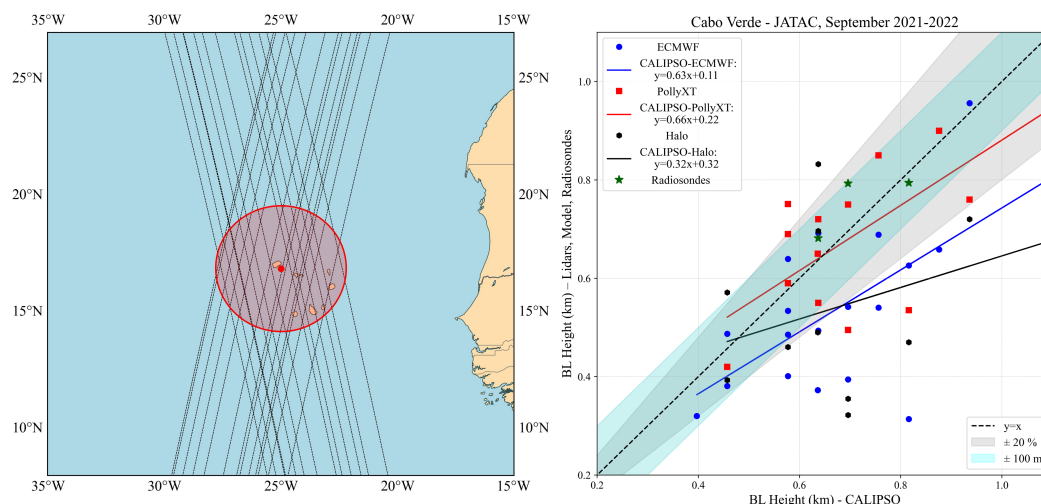


Figure 7. Left: Map showing CALIPSO trajectories (black dashed lines) passing over the ground-based observations site (red point: 16.87°N, 24.99°W) within a 300 km radius (red circle). Right: BL top retrieved from ECMWF (blue points), PollyXT Lidar (red rectangles), Halo Lidar (black hexagons) and Radiosondes (green stars) plotted against the corresponding BL heights from CALIPSO (x-axis). The black dashed line represents the 1:1 line ($y = x$), indicating perfect agreement. The gray shaded area denotes a $\pm 20\%$ error margin, while the cyan shaded region corresponds to a ± 100 m error margin. The correlation lines are given as follows: i) CALIPSO-ECMWF $y = 0.63x + 0.11$ (blue line), ii) CALIPSO-PollyXT $y = 0.66x + 0.22$ (red line), iii) CALIPSO-Halo $y = 0.32x + 0.32$ (black solid line).

The slopes for PollyXT (0.66) and ECMWF (0.63) lines are both below 1, indicating that CALIPSO data present a satisfactory agreement with the model and the ground-based lidar. However, given their small positive intercepts (0.22 and 0.11), these datasets tend to estimate slightly lower BL compared to CALIPSO, even when their trends are generally aligned. The Halo lidar, with the lowest slope (0.32), shows the weakest correlation with CALIPSO. Its larger intercept (0.32) suggests that, while it tends to estimate lower BL heights than CALIPSO, it may show a slight overestimation at lower values of BL. This discrepancy may arise from the different detection methodologies: Halo lidar estimates the MLH using the TKE dissipation rate, whereas the gradient method applied to CALIPSO data primarily identifies layering structures, which may include the entrainment zone or remnants of a residual layer. Similarly, ECMWF use a different retrieval method (thermodynamic approach according to ECMWF, ch. 3). These differences in detection/retrieval methods could also explain why most ECMWF (blue) and Halo (black) points fall below the $y = x$ line, suggesting a potential systematic overestimation of BL height by the space lidar.

3.3.1 Dust Layer above the Marine BL

Figure 8 shows HYSPLIT backward trajectories overlaid on the SST data from the ECMWF/IFS model. The trajectories trace the air masses 48 hours prior to September 12, 2022, at 16:00 (close to the radiosonde launch time), with altitudes at 500 m, 1000 m, and 2600 m. The air at 500 m and 1000 m (black dashed and grey) in Cabo Verde originate over cooler SSTs near



the African shoreline (blue dashed-dotted), while the air from higher levels (2600 m-green) comes from the African continent, likely transporting desert dust.

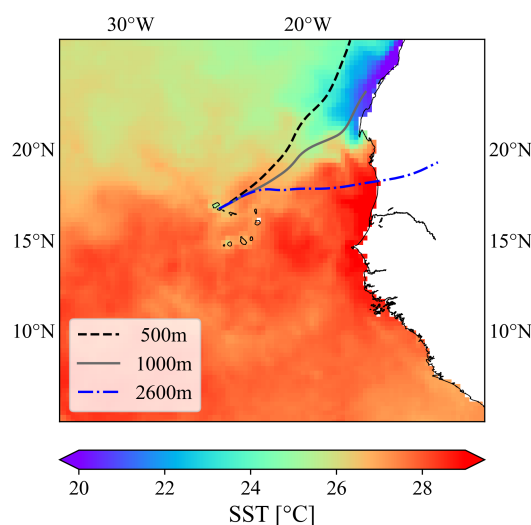


Figure 8. HYSPLIT backward trajectories depict air masses arriving in Mindelo, Cabo Verde, at altitudes of 500 m (black dashed line), 1000 m (grey solid line), and 2600 m (blue dashed-dotted line), 48 hours prior to 16:00 UTC on 12 September 2022, overlaid on ECMWF sea surface temperature (SST) data.

As previously discussed, it is common to observe dust layers transported from Africa to Cabo Verde, creating a distinct layering effect (Carpenter et al., 2010). At lower levels, the marine air mass is in direct contact with the sea surface, while a dust layer lies above it (Tsikoudi et al., 2023). These two layers differ significantly in stability and aerosol composition, resulting in a stratified profile where the dust layer rests on top of the BL. Figure 9a, illustrates the Volume Depolarization Ratio (VLDR) of the 532nm channel from the PollyXT lidar, combined with radiosonde profiles. The greenish colour in the colorbar represents non-spherical aerosols, with depolarization values around 20%, indicative of dust particles. The PollyXT lidar data are plotted for a 30-minute period surrounding the radiosonde launch time (16:19 UTC), ensuring a close temporal match between the two datasets. The relative humidity (blue) and virtual potential temperature (red) profiles from the radiosonde reveal a pronounced inversion near 1 km, aligning well with the stratified layers observed in the depolarization data from the lidar. This inversion acts as a cap, limiting vertical mixing and promoting layer stratification. Additionally, a subtle inversion is present around 500 m in the humidity profile, which may suggest another layered structure. The wind direction (black) remains predominantly northeasterly, with a marked increase in wind speed between 1 and 1.3 km. The BL top, could be signified along the strong humidity inversion, around 1 km. Up to this range, the virtual potential temperature profile (red line) shows instability, continuously decreasing. This indicates that turbulence near the land surface promotes mixing within this layer. This is a typical profile of an unstable layer, where thermal and mechanical eddies near the surface contribute significantly in enhancing mixing. 1 km is quite elevated for a BL in this region, suggesting that local dynamics may be contributing to this

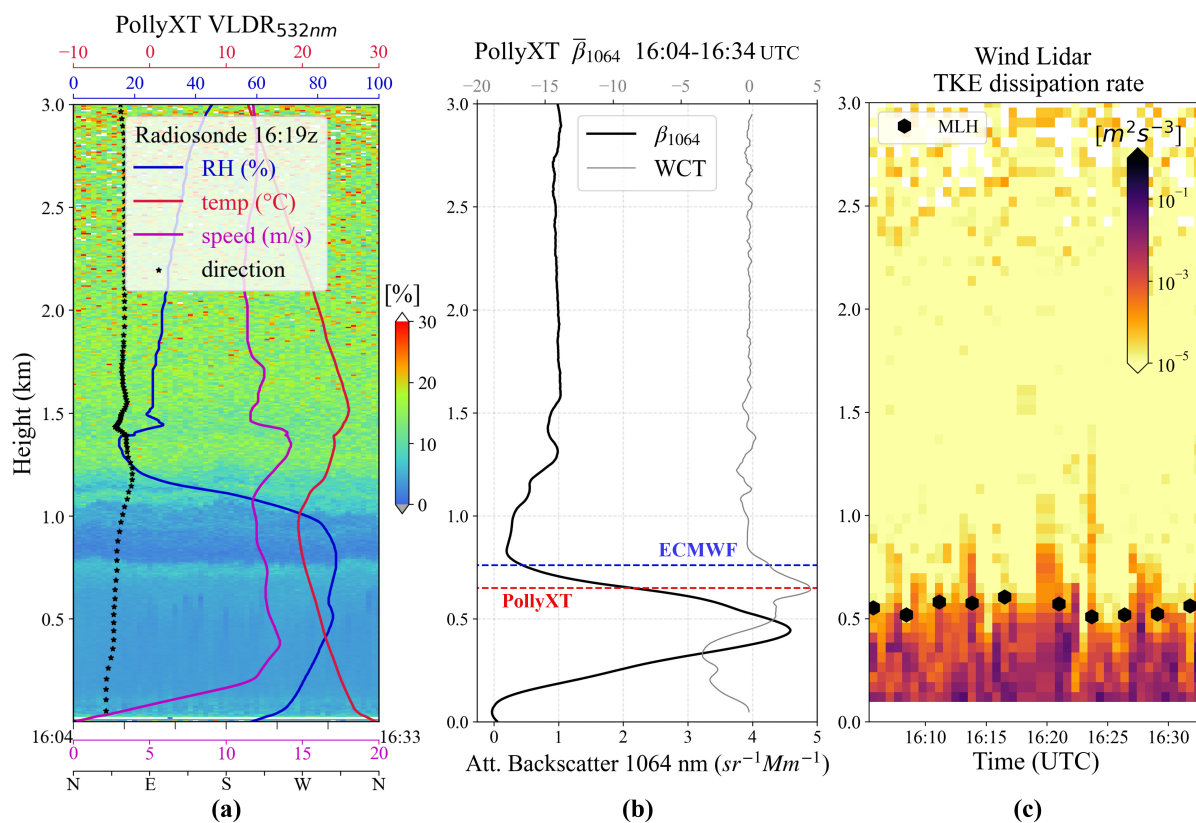


Figure 9. a) Radiosonde profiles for relative humidity (blue), virtual potential temperature (red), wind speed (magenta), and wind direction (black) are plotted over the Volume Depolarization Ratio at 532 nm ($VLDR_{532}$) from the PollyXT lidar, averaged within 30 minutes around the launch time at 16:19 UTC on 12 September 2022 (16:04–16:34 UTC). b) Profile of attenuated backscatter coefficient at 1064 nm (β_{1064}), averaged over the same 30-minute window, with the grey line indicating the WCT, the blue dashed line marking the BL height from ECMWF at 760 m, and the red dashed line highlighting the chosen WCT maximum at 650 m. c) Halo Wind Doppler Lidar Turbulent Kinetic Energy (TKE) dissipation rate for the same 30-minute period. The black hexagons represent the Mixing Layer Height (MLH).



feature. The high wind measured at approximately 13 m/s (≈ 6 Beaufort-magenta color) at about 350 m, introduce strong wind shear and thus considerable mechanical turbulence.

Figure 9b presents the attenuated backscatter coefficient ($\bar{\beta}_{1064}$) profile at 1064 nm from the PollyXT lidar (black line). The profile is averaged over a 30-minute period around the radiosonde launch time (16:24–16:34 UTC). The grey line represents the WCT method, with its maximum indicating a layer top at 650 m (red dashed line). For comparison, the ECMWF BL top at the radiosonde launch time is shown as a blue dashed line at 760 m. The TKE dissipation rate from the Halo Wind Lidar (9c) shows larger values below approximately 520 m, aligning with the identified MLH (black hexagons). This agrees well with the BL top derived from PollyXT (red line in fig. 9b), indicating that both ground-based lidars consistently capture the well-mixed layer.

3.3.2 Desert Dust within the Marine BL

According to the HYSPLIT trajectories in Fig. 10, the air masses arriving over Mindelo at 1000 m and 2000 m altitudes originate from inland Africa, while the lower-level air mass, reaching 500 m, follows a path from the northwest coastline. This again indicates an influx of air masses with distinct characteristics, where the higher layers likely carry Saharan dust, in line with the VLDR measurements of PollyXT Lidar. Additionally, Aerosol Optical Depth (AOD) measurements from the Aerosol Robotic Network (AERONET) for this day report values around 0.6 at 500 nm (data not shown), further supporting the presence of significant dust transport.

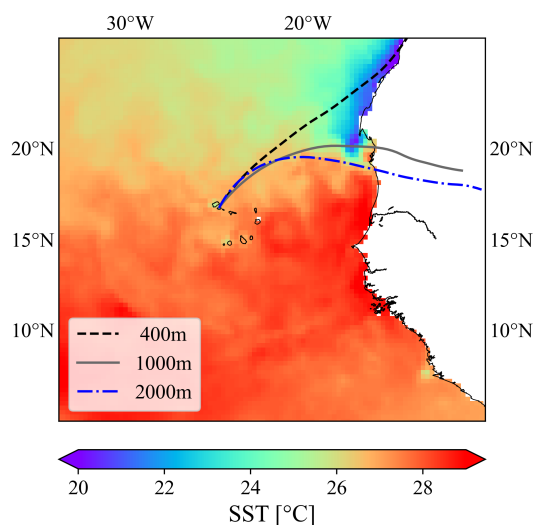


Figure 10. Same as Figure 8 for 23 September 2022. The backward trajectories are calculated at altitudes of 400 m (black dashed line), 1000 m (grey solid line), and 2000 m (blue dashed-dotted line), 48 hours prior to 19:00 UTC on 23 September 2022.

Turbulence at the top of a daytime BL, driven by surface heating and convection, can lead to the entrainment of dust particles from an elevated layer above into the BL (Marsham et al., 2008). In these situations, the dust particles become integrated into



the marine and coastal air masses, impacting aerosol concentrations and BL dynamics. In Figure 11a, the values of VLDR
inside the BL are close to 20%, indicating the existence of dust particles in the MABL, mixed with marine particles. The
radiosonde profiles of virtual potential temperature and relative humidity reveal weaker inversions than those observed in
Section 3.3.1, with a notable inversion around 500 m, which may indicate the approximate BL top in this case. This weakened
inversion also suggests that the BL may be more susceptible to vertical mixing, facilitating dust intrusion from higher altitudes
into the BL. On this particular day, the wind speed profile (magenta line) shows milder conditions, reaching speeds up to 10 m/s
(~5 on the Beaufort scale). The direction of the wind is northern (black stars) relatively to the previous case. At the northern
side of the measurements' site, there is the neighbouring Santo Antão island that could act as an obstacle to the wind's flow,
shaping local dynamics that affect the vertical mixing.

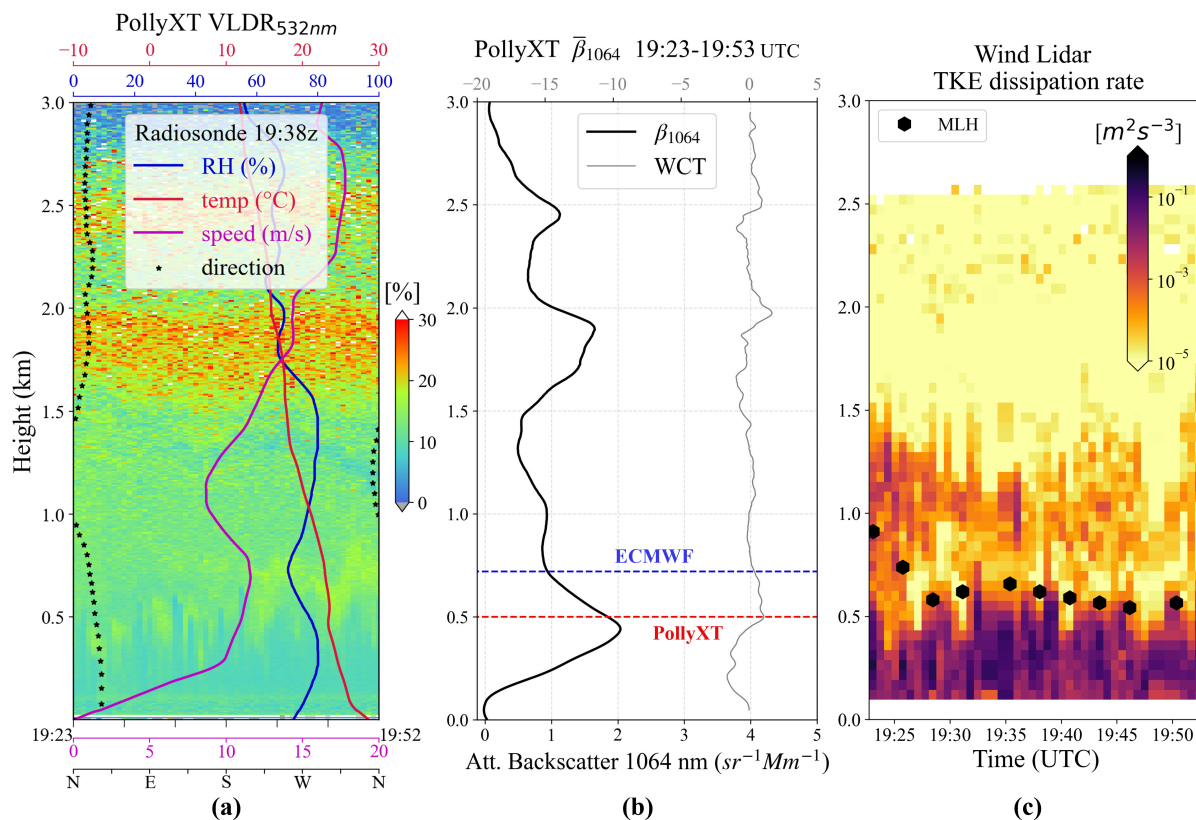


Figure 11. Same as Figure 9 for 23 September 2022. a) The radiosonde launch time at 19:38 UTC on 23 September 2022. b) ECMWF BL height (blue dashed line) at 720 m, WCT maximum (red dashed line) at 500 m. c) Halo Wind Doppler Lidar TKE dissipation rate for the same time period as PollyXT, with the black hexagons representing the MLH.

The WCT method (grey line) applied to the averaged $\bar{\beta}_{1064}$ profile (Fig. 11b) identifies multiple maxima, none of which are particularly dominant. The most pronounced feature below 1.5 km appears at 500 m (red dashed line). This method presents
limitations when the lidar signal is influenced by overlying features, such as elevated aerosol layers or thin cirrus clouds



(Brooks, 2003). In such cases it is essential to cross-check the results with independent measurements. According to Wind lidar TKE dissipation rate, turbulent motions extend up to 600 m (Fig. 11c), while the ECMWF BL top for the same time is located at 720 m (blue dashed line). The two ground-based lidars show better agreement, both indicating a BL top around 500–600 m. The weaker inversion observed in the radiosonde profile supports this lower BL height, however, the ECMWF BL top is notably higher (at 720 m), highlighting a larger discrepancy between the model and observations compared to the previous case.

4 Conclusions

This study highlights the critical importance of understanding the BL in the Atlantic, to better characterize the complex interactions between the ocean and the atmosphere, particularly in the presence of transported Saharan dust. These interactions govern fundamental processes such as evaporation, sea surface temperature variability, and cloud formation, all of which have significant implications for climate modelling and marine ecosystem productivity due to dust nutrient deposition.

Our findings demonstrate that, based on 10 years (2012–2022) of CALIPSO measurements over the open Atlantic (Area 1), the BL height ranges from 600 m to 800 m for both daytime and nighttime trajectories, with cloud-free profiles considered during September. Furthermore, a strong correlation is observed between the CALIPSO measurements and ECMWF/IFS model outputs for this Area during the decade. However, the variations associated with CALIPSO BL are significantly larger than those of the ECMWF/IFS model outputs. CALIPSO's sensitivity to small-scale features such as aerosols and clouds leads to more variability in the data. In contrast, ECMWF/IFS model outputs are based on global atmospheric simulations that provide a more general, smoothed estimate with less sensitivity to local disturbances.

The analysis of Area 2 reveals distinct BL characteristics over the ocean and land, shaped by differences in surface properties, meteorological conditions, and aerosol composition. Over the ocean (35°W–17°W), CALIPSO and ECMWF show strong agreement in BL heights, typically ranging from 500 to 800 meters, consistent with findings from Area 1. However, over the examined area of land (17°W–0°), discrepancies emerge, particularly during the daytime, when ECMWF estimates a significantly higher BL top than CALIPSO, likely due to differences in how the model and lidar capture the mixing layer, residual layer, and entrainment zone. The under-representation of aerosols in ECMWF/IFS model (Morcrette et al., 2008; Bozzo et al., 2020; Rémy et al., 2024) may also contribute to these differences. At night over land, CALIPSO generally reports higher BL than ECMWF, which is most probably due to the presence of the residual layer that provides an aerosol layer height significantly higher than the thermodynamically defined BL top.

In Cabo Verde, collocated data from CALIPSO, PollyXT, Halo Lidar and radiosondes were analyzed for September 2021–2022. Correlations between all measurements and ECMWF with CALIPSO data were assessed. 66% of the PollyXT points, 50% of the ECMWF points and 30% of the Halo points indicate agreement within 20% error when comparing with CALIPSO BL height. The weakest correlation is observed between CALIPSO and Halo Lidar, due to methodological differences —CALIPSO primarily detects layering that may include the residual layer, while Halo Lidar estimates the mixing layer height based on TKE



dissipation rate. Moreover, systematic differences could arise from variations in measurement techniques, retrieval algorithms, or even inherent model biases in representing BL processes.

360 To further investigate the situation in Cabo Verde, two cases with distinct thermodynamic conditions were examined. The first case (12 September 2022) is characterized by stronger inversions and dust aerosols primarily above the capping layer. Temperature and humidity inversions are observed at approximately 1 km; however, PollyXT and Halo Lidar detect the BL top at 650 m and 520 m, respectively, aligning more closely with the marine BL. While the two ground-based lidars show good agreement, the radiosonde profile indicates a higher BL top near 1 km. This discrepancy likely arises because the lidars
365 primarily capture the well-mixed layer, whereas the radiosonde inversion marks a more stable upper boundary, potentially corresponding to the entrainment zone or a decoupled residual layer. Such differences are anticipated in complex environments like Cabo Verde, where the interplay of dust, marine aerosols, and variable meteorological conditions introduce challenges to understand the BL dynamics. In the second case (23 September 2022), characterized by a weaker inversion and dust aerosols within the BL, the BL top was found lower, with both ground-based lidars detecting it around 500 m. The key differences in
370 this case are the smoother wind speed and a more northerly wind direction. The northern wind flow may have been influenced by the presence of Santo Antão island to the north, impacting local dynamics. Additionally, the slope of the virtual potential temperature profile suggests less unstable conditions, promoting better vertical mixing and enabling dust to enter the BL.


The observed differences in BL height can be mainly attributed to the mechanical turbulence driven by strong winds in the first case, highlighting the variability of the atmospheric conditions in this region, that is influenced by a combination of
375 marine and dust aerosols, as well as the complex sea-land interactions in between, that contribute to the diverse atmospheric conditions. SST emerges as a key factor, driving BL evolution, fostering an unstable lower troposphere. This study suggests that when these complex conditions favor less instability, desert dust from the SAL is more efficiently penetrating to the BL. This mechanism should be further examined on its importance as a facilitator of dust deposition to the ocean. Experiments such as JATAC bring the observational synergies needed to study complex BL dynamics governing dust transport.

380 *Data availability.* Visualized datasets of the ASKOS Campaign and additional information are available at <https://askos.space.noa.gr/data>; the ERA5 ECMWF Re-analysis Dataset is available at <https://www.ecmwf.int/en/forecasts/dataset/ecmwf-reanalysis-v5>; the LIVAS CALIPSO data are available upon request.

Author contributions. IT and EM conducted the analysis and drafted the manuscript; MT, EG and VA provided methodological guidance and contributed to the interpretation of the data; EM, MT and VA designed the study framework and defined the research objectives; EP, KR
385 and VV contributed to the data curation, processing, visualization and revisions of the results; EM and VA provided funding acquisition and project administration; All authors edited and reviewed the original draft, provided critical feedback and helped shape the research, analysis and manuscript.



Competing interests. The authors declare that they have no competing interests.

Acknowledgements. This research has been supported by the Hellenic Foundation for Research and Innovation (H.F.R.I.) under the “3rd
390 Call for H.F.R.I. Research Projects to support Post-Doctoral Researchers” (Project Acronym: REVEAL, Project Number: 07222). We also
acknowledge the support by the PANGEA4CalVal project (Grant Agreement 101079201) funded by the European Union . Emmanouil
Proestakis acknowledges support by the AXA Research Fund for postdoctoral researchers under the project entitled “Earth Observation for
Air-Quality – Dust Fine-Mode (EO4AQ-DustFM)”. Funding was also received from Horizon Europe programme under Grant Agreement
No 101137680 via project CERTAINTY (Cloud-aERosol inTeractions & their impActs IN The earth sYstem). Finally, the authors would
395 like to acknowledge the project of ASKOS (Grant agreement 4000131861/20/NL/IA) from the European Space Agency.



References

- Amiridis, V., Marinou, E., Tsekeri, A., Wandinger, U., Schwarz, A., Giannakaki, E., Mamouri, R., Kokkalis, P., Biniotoglou, I., Solomos, S., Herekakis, T., Kazadzis, S., Gerasopoulos, E., Proestakis, E., Kottas, M., Balis, D., Papayannis, A., Kontoes, C., Kourtidis, K., Pappagiannopoulos, N., Mona, L., Pappalardo, G., Le Rille, O., and Ansmann, A.: LIVAS: a 3-D multi-wavelength aerosol/cloud database based on CALIPSO and EARLINET, *Atmospheric Chemistry and Physics*, 15, 7127–7153, <https://doi.org/10.5194/acp-15-7127-2015>, 2015.
- Ansmann, A., Rittmeister, F., Engelmann, R., Basart, S., Jorba, O., Spyrou, C., Remy, S., Skupin, A., Baars, H., Seifert, P., et al.: Profiling of Saharan dust from the Caribbean to western Africa–Part 2: Shipborne lidar measurements versus forecasts, *Atmospheric Chemistry and Physics*, 17, 14987–15006, 2017.
- Atlas, D., Walter, B., Chou, S.-H., and Sheu, P.: The structure of the unstable marine boundary layer viewed by lidar and aircraft observations, *Journal of the atmospheric sciences*, 43, 1301–1318, 1986.
- Baars, H., Ansmann, A., Engelmann, R., and Althausen, D.: Continuous monitoring of the boundary-layer top with lidar, *Atmospheric Chemistry and Physics*, 8, 7281–7296, <https://doi.org/10.5194/acp-8-7281-2008>, 2008.
- Bozzo, A., Benedetti, A., Flemming, J., Kipling, Z., and Rémy, S.: An aerosol climatology for global models based on the tropospheric aerosol scheme in the Integrated Forecasting System of ECMWF, *Geoscientific Model Development*, 13, 1007–1034, 2020.
- Brooks, I. M.: Finding boundary layer top: Application of a wavelet covariance transform to lidar backscatter profiles, *Journal of Atmospheric and Oceanic Technology*, 20, 1092–1105, 2003.
- Carlson, T. N. and Prospero, J. M.: The large-scale movement of Saharan air outbreaks over the northern equatorial Atlantic, *Journal of Applied Meteorology and Climatology*, 11, 283–297, 1972.
- Carpenter, L., Fleming, Z. L., Read, K., Lee, J., Moller, S., Hopkins, J., Purvis, R., Lewis, A., Müller, K., Heinold, B., et al.: Seasonal characteristics of tropical marine boundary layer air measured at the Cape Verde Atmospheric Observatory, *Journal of Atmospheric Chemistry*, 67, 87–140, 2010.
- Croft, B., Martin, R. V., Moore, R. H., Ziemba, L. D., Crosbie, E. C., Liu, H., Russell, L. M., Saliba, G., Wisthaler, A., Müller, M., et al.: Factors controlling marine aerosol size distributions and their climate effects over the Northwest Atlantic Ocean region, *Atmospheric Chemistry and Physics*, 21, 1889–1916, 2021.
- Dunion, J. P. and Velden, C. S.: The impact of the Saharan air layer on Atlantic tropical cyclone activity, *Bulletin of the American Meteorological Society*, 85, 353–366, 2004.
- ECMWF: IFS Documentation CY43R3 - Part IV: Physical processes, 4, ECMWF, <https://doi.org/10.21957/efyk72kl>, 2017.
- Engelmann, R., Kanitz, T., Baars, H., Heese, B., Althausen, D., Skupin, A., Wandinger, U., Komppula, M., Stachlewska, I. S., Amiridis, V., et al.: The automated multiwavelength Raman polarization and water-vapor lidar Polly XT: The neXT generation, *Atmospheric Measurement Techniques*, 9, 1767–1784, 2016.
- Evan, A. T., Vimont, D. J., Heidinger, A. K., Kossin, J. P., and Bennartz, R.: The role of aerosols in the evolution of tropical North Atlantic Ocean temperature anomalies, *Science*, 324, 778–781, 2009.
- Flamant, C., Pelon, J., Flamant, P. H., and Durand, P.: Lidar determination of the entrainment zone thickness at the top of the unstable marine atmospheric boundary layer, *Boundary-Layer Meteorology*, 83, 247–284, 1997.
- Foltz, G. R. and McPhaden, M. J.: Impact of Saharan dust on tropical North Atlantic SST, *Journal of Climate*, 21, 5048–5060, 2008.
- Garcia-Carreras, L., Parker, D., Marsham, J., Rosenberg, P., Brooks, I., Lock, A., Marengo, F., McQuaid, J., and Hobby, M.: The turbulent structure and diurnal growth of the Saharan atmospheric boundary layer, *Journal of the Atmospheric Sciences*, 72, 693–713, 2015.



- Garratt, J. R.: The atmospheric boundary layer, *Earth-Science Reviews*, 37, 89–134, 1994.
- Giménez, J., Pastor, C., Castañer, R., Nicolás, J., Crespo, J., and Carratalá, A.: Influence of Saharan dust outbreaks and atmospheric stability
435 upon vertical profiles of size-segregated aerosols and water vapor, *Atmospheric Environment*, 44, 338–346, 2010.
- Hanson, H. P.: Marine stratocumulus climatologies, *International journal of climatology*, 11, 147–164, 1991.
- Hunt, W. H., Winker, D. M., Vaughan, M. A., Powell, K. A., Lucker, P. L., and Weimer, C.: CALIPSO lidar description and performance
assessment, *Journal of Atmospheric and Oceanic Technology*, 26, 1214–1228, 2009.
- Kallos, G., Astitha, M., Katsafados, P., and Spyrou, C.: Long-range transport of anthropogenically and naturally produced particulate matter
440 in the Mediterranean and North Atlantic: Current state of knowledge, *Journal of Applied Meteorology and Climatology*, 46, 1230–1251,
2007.
- Li, H., Liu, B., Ma, X., Jin, S., Ma, Y., Zhao, Y., and Gong, W.: Evaluation of retrieval methods for planetary boundary layer height based on
radiosonde data, *Atmospheric Measurement Techniques*, 14, 5977–5986, 2021.
- Li, Z., Guo, J., Ding, A., Liao, H., Liu, J., Sun, Y., Wang, T., Xue, H., Zhang, H., and Zhu, B.: Aerosol and boundary-layer interactions and
445 impact on air quality, *National Science Review*, 4, 810–833, 2017.
- Liu, B., Ma, Y., Liu, J., Gong, W., Wang, W., and Zhang, M.: Graphics algorithm for deriving atmospheric boundary layer heights from
CALIPSO data, *Atmospheric Measurement Techniques*, 11, 5075–5085, 2018.
- Liu, Z., Vaughan, M., Winker, D., Kittaka, C., Getzewich, B., Kuehn, R., Omar, A., Powell, K., Treppe, C., and Hostetler, C.: The CALIPSO
lidar cloud and aerosol discrimination: Version 2 algorithm and initial assessment of performance, *Journal of Atmospheric and Oceanic*
450 *Technology*, 26, 1198–1213, 2009.
- Luo, B., Minnett, P. J., Zuidema, P., Nalli, N. R., and Akella, S.: Saharan Dust Effects on North Atlantic Sea-Surface Skin Temperatures,
Journal of Geophysical Research: Oceans, 126, e2021JC017 282, 2021.
- Marinou, E., Amiridis, V., Biniotoglou, I., Tsikerdekis, A., Solomos, S., Proestakis, E., Konsta, D., Papagiannopoulos, N., Tsekeri, A.,
Vlastou, G., et al.: Three-dimensional evolution of Saharan dust transport towards Europe based on a 9-year EARLINET-optimized
455 CALIPSO dataset, *Atmospheric Chemistry and Physics*, 17, 5893–5919, 2017.
- Marinou, E., Voudouri, K. A., Tsikoudi, I., Drakaki, E., Tsekeri, A., Rosoldi, M., Ene, D., Baars, H., O'Connor, E., Amiridis, V., et al.:
Geometrical and microphysical properties of clouds formed in the presence of dust above the Eastern Mediterranean, *Remote Sensing*,
13, 5001, 2021.
- Marinou, E., Paschou, P., Tsikoudi, I., Tsekeri, A., Daskalopoulou, V., Kouklaki, D., Siomos, N., Spanakis-Misirlis, V., Voudouri, K. A.,
Georgiou, T., et al.: An overview of the ASKOS campaign in Cabo Verde, *Environmental Sciences Proceedings*, 26, 200, 2023.
- Marsham, J. H., Parker, D. J., Grams, C. M., Johnson, B. T., Grey, W. M., and Ross, A. N.: Observations of mesoscale and boundary-layer
scale circulations affecting dust transport and uplift over the Sahara, *Atmospheric Chemistry and Physics*, 8, 6979–6993, 2008.
- Menut, L., Masson, O., and Bessagnet, B.: Contribution of Saharan dust on radionuclide aerosol activity levels in Europe? The 21–22
February 2004 case study, *Journal of Geophysical Research: Atmospheres*, 114, 2009.
- 465 Morcrette, J.-J., Beljaars, A., Benedetti, A., Jones, L., and Boucher, O.: Sea-salt and dust aerosols in the ECMWF IFS model, *Geophysical*
Research Letters, 35, 2008.
- O'Connor, E. J., Illingworth, A. J., Brooks, I. M., Westbrook, C. D., Hogan, R. J., Davies, F., and Brooks, B. J.: A method for estimating the
turbulent kinetic energy dissipation rate from a vertically pointing Doppler lidar, and independent evaluation from balloon-borne in situ
measurements, *Journal of atmospheric and oceanic technology*, 27, 1652–1664, 2010.



- 470 Pearson, G., Davies, F., and Collier, C.: An analysis of the performance of the UFAM pulsed Doppler lidar for observing the boundary layer, *Journal of Atmospheric and Oceanic Technology*, 26, 240–250, 2009.
- Pena, A., Gryning, S.-E., and Floors, R. R.: Lidar observations of marine boundary-layer winds and heights: a preliminary study, *Meteorologische Zeitschrift*, 24, 581–589, 2015.
- Pérez, C., Nickovic, S., Baldasano, J., Sicard, M., Rocadenbosch, F., and Cachorro, V.: A long Saharan dust event over the western Mediter-
475 ranean: Lidar, Sun photometer observations, and regional dust modeling, *Journal of Geophysical Research: Atmospheres*, 111, 2006.
- Proestakis, E., Gkikas, A., Georgiou, T., Kampouri, A., Drakaki, E., Ryder, C. L., Marengo, F., Marinou, E., and Amiridis, V.: A near-global multiyear climate data record of the fine-mode and coarse-mode components of atmospheric pure dust, *Atmospheric Measurement Techniques*, 17, 3625–3667, 2024.
- Prospero, J. M. and Mayol-Bracero, O. L.: Understanding the transport and impact of African dust on the Caribbean Basin, *Bulletin of the*
480 *American Meteorological Society*, 94, 1329–1337, 2013.
- Rémy, S., Kipling, Z., Flemming, J., Boucher, O., Nabat, P., Michou, M., Bozzo, A., Ades, M., Huijnen, V., Benedetti, A., et al.: Description and evaluation of the tropospheric aerosol scheme in the European Centre for Medium-Range Weather Forecasts (ECMWF) Integrated Forecasting System (IFS-AER, cycle 45R1), *Geoscientific Model Development*, 12, 4627–4659, 2019.
- Rémy, S., Kipling, Z., Huijnen, V., Flemming, J., Nabat, P., Michou, M., Ades, M., Engelen, R., and Peuch, V.-H.: Description and evalu-
485 ation of the tropospheric aerosol scheme in the Integrated Forecasting System (IFS-AER, cycle 47R1) of ECMWF, *Geoscientific Model Development Discussions*, 2021, 1–44, 2021.
- Rémy, S., Metzger, S., Huijnen, V., Williams, J. E., and Flemming, J.: An improved representation of aerosol in the ECMWF IFS-COMPO 49R1 through the integration of EQSAM4Climv12—a first attempt at simulating aerosol acidity, *Geoscientific Model Development*, 17, 7539–7567, 2024.
- 490 Rolph, G., Stein, A., and Stunder, B.: Real-time environmental applications and display system: READY, *Environmental Modelling & Software*, 95, 210–228, 2017.
- Schnitker, D.: Climatic variability and deep ocean circulation: evidence from the North Atlantic, *Palaeogeography, Palaeoclimatology, Palaeoecology*, 40, 213–234, 1982.
- Seibert, P., Beyrich, F., Gryning, S.-E., Joffre, S., Rasmussen, A., and Tercier, P.: Review and intercomparison of operational methods for the
495 determination of the mixing height, *Atmospheric environment*, 34, 1001–1027, 2000.
- Seidel, D. J., Zhang, Y., Beljaars, A., Golaz, J.-C., Jacobson, A. R., and Medeiros, B.: Climatology of the planetary boundary layer over the continental United States and Europe, *Journal of Geophysical Research: Atmospheres*, 117, 2012.
- Stephens, G., Winker, D., Pelon, J., Trepte, C., Vane, D., Yuhas, C., L’ecuyer, T., and Lebsock, M.: CloudSat and CALIPSO within the A-Train: Ten years of actively observing the Earth system, *Bulletin of the American Meteorological Society*, 99, 569–581, 2018.
- 500 Stull, R. B.: Mean boundary layer characteristics, in: *An introduction to boundary layer meteorology*, pp. 1–27, Springer, 1988.
- Sun, Y. and Zhao, C.: Influence of Saharan dust on the large-scale meteorological environment for development of tropical cyclone over North Atlantic Ocean Basin, *Journal of Geophysical Research: Atmospheres*, 125, e2020JD033 454, 2020.
- Tackett, J. L., Winker, D. M., Getzewich, B. J., Vaughan, M. A., Young, S. A., and Kar, J.: CALIPSO lidar level 3 aerosol profile product: Version 3 algorithm design, *Atmospheric Measurement Techniques*, 11, 4129–4152, 2018.
- 505 Tombrou, M., Dandou, A., Helmis, C., Akylas, E., Angelopoulos, G., Flocas, H., Assimakopoulos, V., and Soulakellis, N.: Model evaluation of the atmospheric boundary layer and mixed-layer evolution, *Boundary-layer meteorology*, 124, 61–79, 2007.



- Tombrou, M., Bossioli, E., Kalogiros, J., Allan, J., Bacak, A., Biskos, G., Coe, H., Dandou, A., Kouvarakis, G., Mihalopoulos, N., et al.: Physical and chemical processes of air masses in the Aegean Sea during Etesians: Aegean-GAME airborne campaign, *Science of the Total Environment*, 506, 201–216, 2015.
- 510 Tsaknakis, G., Papayannis, A., Kokkalis, P., Amiridis, V., Kambezidis, H., Mamouri, R., Georgoussis, G., and Avdikos, G.: Inter-comparison of lidar and ceilometer retrievals for aerosol and Planetary Boundary Layer profiling over Athens, Greece, *Atmospheric Measurement Techniques*, 4, 1261–1273, 2011.
- Tsikoudi, I., Marinou, E., Vakkari, V., Gialitaki, A., Tsichla, M., Amiridis, V., Komppula, M., Raptis, I. P., Kampouri, A., Daskalopoulou, V., et al.: PBL height retrievals at a coastal site using multi-instrument profiling methods, *Remote Sensing*, 14, 4057, 2022.
- 515 Tsikoudi, I., Marinou, E., Voudouri, K., Koutsoupi, I., Drakaki, E., Kampouri, A., Vakkari, V., Baars, H., Giannakaki, E., Tombrou, M., et al.: PBL Height Retrievals during ASKOS Campaign, *Environmental Sciences Proceedings*, 26, 23, 2023.
- Vakkari, V., O’connor, E., Nisantzi, A., Mamouri, R., and Hadjimitsis, D.: Low-level mixing height detection in coastal locations with a scanning Doppler lidar, *Atmospheric Measurement Techniques*, 8, 1875–1885, 2015.
- Vakkari, V., Manninen, A. J., O’Connor, E. J., Schween, J. H., Van Zyl, P. G., and Marinou, E.: A novel post-processing algorithm for Halo
520 Doppler lidars, *Atmospheric Measurement Techniques*, 12, 839–852, 2019.
- Vaughan, M. A., Powell, K. A., Winker, D. M., Hostetler, C. A., Kuehn, R. E., Hunt, W. H., Getzewich, B. J., Young, S. A., Liu, Z., and McGill, M. J.: Fully automated detection of cloud and aerosol layers in the CALIPSO lidar measurements, *Journal of Atmospheric and Oceanic Technology*, 26, 2034–2050, 2009.
- Vogelezang, D. and Holtzlag, A.: Evaluation and model impacts of alternative boundary-layer height formulations, *Boundary-Layer Meteorology*, 81, 245–269, 1996.
- 525 Wiegner, M., Emeis, S., Freudenthaler, V., Heese, B., Junkermann, W., Munkel, C., Schäfer, K., Seefeldner, M., and Vogt, S.: Mixing layer height over Munich, Germany: Variability and comparisons of different methodologies, *Journal of Geophysical Research: Atmospheres*, 111, 2006.
- Winker, D., Pelon, J., Coakley Jr, J., Ackerman, S., Charlson, R., Colarco, P., Flamant, P., Fu, Q., Hoff, R., Kittaka, C., et al.: The CALIPSO mission: A global 3D view of aerosols and clouds, *Bulletin of the American Meteorological Society*, 91, 1211–1230, 2010.
- 530 Winker, D., Tackett, J., Getzewich, B., Liu, Z., Vaughan, M., and Rogers, R.: The global 3-D distribution of tropospheric aerosols as characterized by CALIOP, *Atmospheric Chemistry and Physics*, 13, 3345–3361, 2013.
- Wood, R.: Stratocumulus clouds, *Monthly Weather Review*, 140, 2373–2423, 2012.
- Wu, L.: Impact of Saharan air layer on hurricane peak intensity, *Geophysical research letters*, 34, 2007.
- 535 Yu, H., Kaufman, Y., Chin, M., Feingold, G., Remer, L., Anderson, T., Balkanski, Y., Bellouin, N., Boucher, O., Christopher, S., et al.: A review of measurement-based assessments of the aerosol direct radiative effect and forcing, *Atmospheric Chemistry and Physics*, 6, 613–666, 2006.
- Zeng, S., Vaughan, M., Liu, Z., Trepte, C., Kar, J., Omar, A., Winker, D., Lucker, P., Hu, Y., Getzewich, B., et al.: Application of high-dimensional fuzzy k-means cluster analysis to CALIOP/CALIPSO version 4.1 cloud–aerosol discrimination, *Atmospheric Measurement
540 Techniques*, 12, 2261–2285, 2019.
- Zhou, W., Leung, L. R., Lu, J., Yang, D., and Song, F.: Contrasting recent and future ITCZ changes from distinct tropical warming patterns, *Geophysical Research Letters*, 47, e2020GL089 846, 2020.